Concentration and composition of the protein corona as a function of incubation time and serum concentration: An automated approach to the protein corona

Karsten M. Poulsen and Christine K. Payne*

Thomas Lord Department of Mechanical Engineering and Materials Science, Duke University, Durham, North Carolina, USA 27705

christine.payne@duke.edu

Abstract

Nanoparticles in contact with proteins form a “corona” of proteins adsorbed on the nanoparticle surface. Subsequent biological responses are then mediated by the adsorbed proteins rather than the bare nanoparticles. The use of nanoparticles as nanomedicines and biosensors would be greatly improved if researchers were able to predict which specific proteins will adsorb on a nanoparticle surface. We use a recently developed automated workflow with a liquid handling robot and low-cost proteomics to determine the concentration and composition of the protein corona formed on carboxylate-modified iron oxide nanoparticles (200 nm) as a function of incubation time and serum concentration. We measure the concentration of the resulting protein corona with a colorimetric assay and the composition of the corona with proteomics, reporting both abundance and enrichment relative to the fetal bovine serum (FBS) proteins used to form the corona. Incubation time was found to be an important parameter for corona concentration and composition at high (100% FBS) incubation concentrations, with only a slight effect at low (10%) FBS concentrations. In addition to these findings, we describe two methodological advances to help reduce the cost associated with protein corona experiments. We have automated the digest step necessary for proteomics and measured the variability between triplicate samples at each stage of the proteomics experiments. Overall, these results demonstrate the importance of understanding the multiple parameters that influence corona formation, provide new tools for corona characterization, and advance bioanalytical research in nanomaterials.

Introduction

Nanoparticles (NPs) present in any biological environment are exposed to proteins that adsorb on the NP surface forming a protein corona. This protein corona determines the biological identity of the NP, controlling cellular internalization, immune response, biodistribution, and circulation time [1-12]. A better understanding of the protein corona is essential for both effective development of nanomedicines and nanosensors and determination of the toxicity associated with human exposure to NPs [13-16]. The varied properties of NPs (diameter, composition, zeta potential, surface functionalization), the complexity of biological systems (protein structure, hydrophobicity, and charge; concentration of biomolecules), and the effect of the methods used to prepare and analyze the corona makes it difficult to unravel the relevant parameters that control the NP-protein interaction [2, 6, 17, 18]. For example, recent work has highlighted that even the specific type of mixing process used to form the corona; rocking, vortexing, or flow, will alter the protein corona [19]. Similarly, separation of the protein-NP complexes from unbound protein by centrifugation or magnetic separation will result in a different protein corona [20, 21].

To advance the field, we need to move to larger data sets and improved reproducibility, while also considering cost and accessibility of experiments [22, 23]. For example, liquid chromatography tandem mass spectrometry (LC-MS/MS) is necessary for corona analysis, but it is an expensive technique that requires access to a proteomics core facility. Gel electrophoresis is much less expensive, but often requires LC-MS/MS or western blotting for verification. Obtaining the maximum amount of information from gel electrophoresis experiments would help reduce the costs of protein corona experiments [23]. Machine learning offers the exciting possibility of being able to predict the composition of the protein corona on a given NP, thereby reducing the costs associated with experiments. Existing efforts have focused on protein properties [24-26]. Future work focusing on NP properties would further advance the field. The large data sets required for these experiments will require automated formation, isolation, and analysis of the protein corona. In addition to increasing the number of samples, automation will save time and costs, and improve reproducibility [22, 27].

We describe the concentration and composition of the protein corona as a function of incubation time (30 min and 1 day) and the concentration of fetal bovine serum (FBS) used to form the corona (5%, 10%, and 100%) on 200 nm carboxylate-modified magnetic NPs, using semi-automated processes. The isolated protein-NP complexes were analyzed using dynamic light scattering (DLS), a bulk protein colorimetric assay, gel electrophoresis, and LC-MS/MS. To understand the need, and costs, for replicates in LC-MS/MS studies, sample replicates were compared at each step of the process. Our experiments show that incubation time is an important parameter for corona concentration, but only at high (100% FBS) incubation concentrations. Quantifying the enrichment and depletion of corona proteins relative to the FBS used to form the corona provides a compositional signature of the protein corona that points us toward protein features that influence corona formation, identifying individual proteins for future studies. Proteomics data shows a shifting composition of corona proteins as a function of

incubation time and concentration, but mostly of low abundance proteins. In addition to this corona characterization, we describe a protocol for the automation of the digest step necessary for proteomics. We hope these results will clarify the importance of incubation time and concentration as interdependent variables in corona formation and help to advance corona experiments by reducing the costs.

Materials and Methods

Nanoparticles (NPs)

Magnetic nanoparticles (200 nm, carboxylate-modified, #SC0202, Ocean NanoTech, San Diego, CA) were used for all experiments.

NP characterization

NP diameter was measured with transmission electron microscopy (TEM) and dynamic light scattering (DLS). TEM was carried out using Tecnai G² TWIN TEM (FEI, Hillsboro, OR) at the Shared Materials Instrumentation Facility at Duke University. NP images were obtained at 160 kV with 25 kX magnification. All samples were prepared by drop casting on 400 mesh copper grids (#CF400-Cu, Electron Microscopy Sciences, Hatfield Township, PA) and drying at room temperature (RT) for 12-18 hrs. Nanoparticle diameters were measured using ImageJ [28]. Average and standard deviation are reported for all measurements.

Hydrodynamic diameter, polydispersity index, and zeta potential of the NPs (100 µg/mL in phosphate buffered saline (PBS) diluted 1:100 in ultrapure water) were measured using DLS (Zetasizer, Malvern Instruments, Worcestershire, England). Measurements were carried out in triplicate with three distinct samples. Each measurement was performed for 12 - 30 runs. The average and standard deviation are reported for all measurements. Electrophoretic mobility was converted to zeta potential using the Smoluchowski approximation.

Liquid handling robot

A liquid handling robot (OT-2, Opentrons, Brooklyn, NY) with a magnetic baseplate and temperature-control module was used to automate protein corona formation and isolation, as described previously [22]. Protocol scripts were written in python using Opentrons API v2.11. Pipette tips (300 µl, single and multi) and tip racks were purchased from Opentrons to verify compatibility and calibration. The locations of each reagent and sample were designated in the script and appropriately positioned prior to running the robot. Most experiments used a 96-well plate with three or six replicates, specified in the text. Within a row of eight wells, two wells were used for background subtraction.

Protein corona formation and quantification

A protein corona was formed by incubating NPs (3.2 mg/mL) in 1-100% solutions of FBS (#10437028, Thermo Fisher Scientific, Waltham, MA) diluted in PBS. The incubations were performed at RT on a microplate shaker for times ranging from 30 minutes to 1 day, as specified in the text. To remove unbound proteins, the NPs were “washed” by the robot. Each wash step consisted of a magnetic pull down using the magnetic baseplate,

removal of the supernatant, and then resuspension in an equal volume of PBS. The hard corona is defined as the protein that remains bound to the NPs with no unbound protein detected in the supernatant, as described below. Centrifugation is typically used for removal of unbound proteins. The use of magnetic pulldown with the liquid handling robot provides a faster workflow [22]. The number of washes required to remove unbound protein was dependent on the concentration of FBS used for corona formation (Fig. S1).

Protein concentration was measured with the Pierce 660 nm Protein Assay Reagent (referred to as a 660 nm assay; #2260, Thermo Fisher Scientific) with the addition of Ionic Detergent Compatibility Reagent (#22663, Thermo Fisher Scientific) according to the manufacturer's instructions. The concentration of protein present in the hard corona was determined by removing the proteins from the NPs by incubating with sodium dodecyl sulfate (SDS) buffer (5% w/v, #L3771, Sigma-Aldrich, Burlington, MA) for 30 minutes at RT. Protein concentration was then determined by measuring absorbance at 660 nm using a plate reader (Spectramax iD3, Molecular Devices, San Jose, CA). A residual amount of protein is resistant to SDS removal independent of duration of SDS incubation (Fig. S2). The NP concentration after the washing process was measured by absorption at 440 nm and comparison with a calibration curve of known concentrations. Protein concentration is reported as protein relative to NP concentration (μg protein/mg NPs).

Protein digestion for proteomics

Prior to proteomic analysis, samples were digested using a modified S-Trap mini column (Protifi, Farmingdale, NY) protocol. Proteins were removed from the NP surface by incubating with SDS buffer for 30 minutes. Protein concentration was determined using the 660 nm assay. Samples were pooled to load a minimum of 25 μg of protein on each S-Trap. Two modifications were made to the S-trap protocol: dithiothreitol (DTT; #R0861, Thermo Fisher Scientific) and iodoacetamide (IAM; #I1149, Sigma-Aldrich) were used as the reducer (20 mM) and alkylator (40 mM), respectively. DTT and IAM are commonly used for proteomics and are recommended substitutions. Following the completion of the S-trap protocol the resulting digested proteins were lyophilized and stored at -20 °C until proteomic analysis.

Proteomic analysis

Proteomic analysis was carried out in the Proteomics and Metabolomics Core Facility, part of the Duke Center for Genomics and Computational Biology, as described previously [22]. In brief, digested samples were analyzed using LC-MS/MS with ≤ 25 μg of digested protein injected. MicroFlow LC was performed with an ultra-performance liquid chromatography (UPLC, 1 mm x 100 mm, M-Class, Waters Corporation; 80 μL/min) column and a 17 minute total elution time. The column was run with an acetonitrile gradient (5-40%) with 0.1% formic acid. Peptide fragments were analyzed using in-line tandem mass spectrometry (Orbitrap Fusion Lumos, Thermo Fisher).

To further develop our low-cost workflow, we analyzed the LC-MS/MS data using MaxQuant (v2.1.0, Max Plank Institute, Munich, Germany), an open source software designed to qualitatively and quantitatively analyze mass spectrometry data [29, 30]. The

raw LC-MS/MS spectra were searched, using their integrated Andromeda search engine, against the Swiss-Prot Bos Taurus canonical protein database from UniProt, accessed on April 27, 2022. A custom contaminants file was used while searching, which contained a relevant subset of the Common Repository of Adventitious Proteins (cRAP) database [31]. For protein and peptide quantification and identification, default MaxQuant parameters were used including a 0.01 false discovery rate, a minimum peptide length of 7 amino acids, a maximum peptide length of 25 amino acids, oxidation and acetyl groups as variable modifications, and carbamidomethyl as a fixed modification. The Top3 label-free protein quantification method was used, as described previously for shotgun proteomic studies of the protein corona [32-34]. This quantification method averages the integrated intensity of the three most intense peptides for each protein.

Resulting proteomic data was analyzed and filtered in Perseus (v2.0.3.1, Max Plank Institute). Proteins were excluded if they were considered contaminants, quality control standards, or were not observed in at least 70% of the samples. This 70% requirement, the default for Perseus, is appropriate for similar samples such as these. After filtering in Perseus, 205 proteins were observed across 15 different samples. Data normalization, heatmap and Venn diagram generation were performed in Python (v3.9, Python Software Foundation, Beaverton, OR). A quantitative internal standard was not used for these experiments. Low abundance proteins in serum, defined as less than 3 peptides observed, had abundances set to 3% of the lowest observed abundance, which allowed fold change to be calculated. To correct for any change in performance or differences in protein loading, each sample was normalized to itself by dividing by the mean of the interior 80% of the protein intensities [35]. Each sample was scaled to have the same average. We report these values as percent normalized abundance. Fold change for each protein was calculated by taking the log base 2 of the normalized abundance of samples divided by serum.

Our discussion focuses on the 50 most abundant proteins present in the coronas. The total number of observed proteins is larger: 205 proteins were observed in the protein corona formed from a 30 min, 10% FBS incubation condition and 60 proteins were identified in FBS. Based on the concentration of protein per NP in the 30 min, 10% FBS sample, we estimate 1,200 proteins are present on each NP. This calculation uses the molecular weight of albumin as a representative protein. Albumin is the most abundant protein in the corona and its molecular weight is near the weighted average of the other corona proteins, making it an appropriate representative protein. Proteins with a normalized abundance of >0.3%, and therefore not one of the 50 most abundant proteins, are calculated to be present at levels less than 4 proteins per NP. At this low level, we assume these low abundance proteins are not drivers of biological responses. The complete lists of proteins are included in the Electronic Supplementary Material (ESM; Table S1). In addition, the mass spectrometry proteomics data have been deposited to the ProteomeXchange Consortium via the Proteomics Identification Database (PRIDE) partner repository with the dataset identifier PXDxxxxx and DOI xxxxxx/PXDxxxxx [36].

Gel electrophoresis

Gel electrophoresis was used to visualize individual proteins present in the corona of the NPs, as described previously [22]. In brief, protein coronas were removed from NPs using SDS, as described above. The removed proteins were heated in loading buffer (Laemmli, #BP-110R; Boston BioProducts, Ashland, MA), incubated for 5 min at 95°C, and loaded onto a gel (tris-glycine sodium dodecyl sulfate (SDS) gel, #4561093, Bio-Rad, Hercules, CA) for SDS-polyacrylamide gel electrophoresis (PAGE; 230 V, 35 min). A 10 to 250 kDa molecular weight marker (Precision Plus Protein Dual Color Standards, #1610374, Bio-Rad) was included. Gels were rinsed by microwaving in deionized water (1 min heat, 1 min rocking at RT, replace water, x3), stained (SimplyBlue Safe Stain, #LC6060, Thermo Fisher) by microwaving until near boiling (1 min), and then rocked for 5 min. Gels were destained in deionized water (10 min, rocking) and NaCl solution (20% w/v, >5 minutes, rocking) and then imaged (PhotoDoc-It, Analytik Jena, Jena, Germany).

Results and Discussion

NP characterization

Commercially-available magnetic NPs (200 nm, carboxylate-modified) were used for all experiments. They were characterized by TEM and DLS (Table 1) prior to experiments. The use of commercial NPs allows other researchers easy access to these materials. Magnetic NPs and a magnetic baseplate are necessary for high-throughput experiments using the liquid handling robot. Without magnetic separation, NPs require centrifugation to separate NPs from unbound proteins. Centrifugation is a bottleneck in the standard protein corona workflow as NPs are moved to the centrifuge and multiple centrifugation and resuspension steps are required.

Protein corona increases NP diameter and zeta potential

Protein coronas were formed by incubating NPs in FBS. FBS is used as a nutrient source for many cell lines. The concentrations of FBS used to form the protein corona ranged from 1%-100%, as specified in the text. 100% FBS, equivalent to 40 mg/mL of protein as measured by a 660 nm assay, was used to model *in vivo* protein concentrations. Since cells are typically cultured in 10% FBS, 10% FBS was used to model *in vitro* protein concentrations. A hard corona was defined as the protein adsorbed to the surface of the NPs after no unbound protein is present in the supernatant, as determined by a 660 nm protein assay. This required 6 wash steps for NPs incubated with 10% FBS and 12 wash steps for NPs incubated with 100% FBS (Fig. S1).

Following incubation with 10% or 100% FBS (30 min, RT), the hard corona significantly increased the hydrodynamic diameter (d_h) and zeta potential of the resulting protein-NP complexes, as determined by a one-way analysis of variance (ANOVA) with a post-hoc Tukey test ($p<0.01$), in comparison to the bare NPs. These changes are in agreement with previous work in our lab [37-40], and others [2, 41-44]. For example, an extensive study of 105 different gold NPs (15 nm, 30 nm, and 60 nm cores; 67 different anionic, cationic, and neutral ligands) showed a similar increase in d_h following corona formation [44]. The change in zeta potential depends on the initial charge of the NP. Both cationic

and anionic NPs form a protein corona. The zeta potential of the protein-NP complex will reflect the charge of adsorbed protein. For example, comparing cationic (amine-modified) and anionic (carboxlylate-modified) polystyrene NPs (200 nm) showed that cationic NPs become anionic following formation of a protein corona and anionic NPs show an increased zeta potential, becoming less negative [37].

Table 1 NP diameter (d_{TEM} and d_h), polydispersity index (PDI), and zeta potential (ZP).

d_{TEM} (nm)	[FBS] (%)	d_h (nm)	PDI	Δd_h (nm)	ZP (mV)	ΔZP (mV)
129 ± 43	0	242 ± 4	0.13 ± 0.004	-	-39 ± 1	-
-	10	305 ± 17	0.17 ± 0.04	+63	-34 ± 2	+5
-	100	313 ± 15	0.19 ± 0.05	+71	-33 ± 2	+6

Concentration of the protein corona increases with FBS concentration

The concentration of the protein corona is measured with a colorimetric assay (660 nm assay). We report protein corona concentration (μg)/NP concentration (mg), as described in Materials and Methods. We observed that the amount of protein adsorbed on the NP surface increases as the initial concentration of FBS used to form the corona increases (1% to 100%; Fig. 1a). For these experiments, the incubation time was kept constant at 30 min, a standard incubation time for corona experiments [45, 46]. All experiments were carried out at RT.

Previous studies have examined corona concentration as a function of the concentration of serum used to form the corona [43, 47, 48]. While many of these studies have also observed an increase in corona concentration as a function of serum concentration, it is important to note that this result depends on NP composition and type of serum. For example, a side-by-side comparison of silica and polystyrene NPs, both 200 nm, in human plasma (1 hr incubation, 3%-80% plasma) showed an increasing corona on the polystyrene NPs, but a slightly decreasing corona on the silica NPs, with increasing plasma concentrations [43]. A comparison of corona formation on poly(lactide-co-glycolide) NPs (200 nm; 30 min incubation) using human serum and FBS showed different adsorption isotherms for the two different serums [47].

Increasing incubation time increases the concentration of the protein corona: Greater increase at high (100%) FBS incubation concentrations

In a second set of experiments, we varied incubation time (30 min or 1 day) and kept the initial FBS incubation concentration constant at 10% FBS or 100% FBS. For coronas formed with 10% FBS, increasing the incubation time resulted in only a small (15%) increase in the amount of protein adsorbed on the NP surface (Fig. 1b). In comparison, incubation with 100% FBS resulted in an increased (59%) corona concentration following a 1 day incubation in FBS (Fig. 1b). Much previous work has addressed the time dependence of corona formation including the concentration and composition of adsorbed proteins [41, 49-52]. Despite extensive study, it has been difficult to identify a general trend in time-dependent changes in protein corona concentration. For example, a

comparison of human plasma protein adsorption on cationic polystyrene NPs (120 nm), anionic polystyrene NPs (120 nm), and anionic silica NPs (35 nm) from 1-1000 min showed an overall increase with time for the anionic NPs, both polystyrene and silica, but with different rates. Cationic polystyrene NPs showed a loss in protein over time. Separate experiments with anionic mesoporous silica NPs (100 nm) showed an increase in protein concentration when incubated with human serum or FBS over a 1-10,000 min period [52].

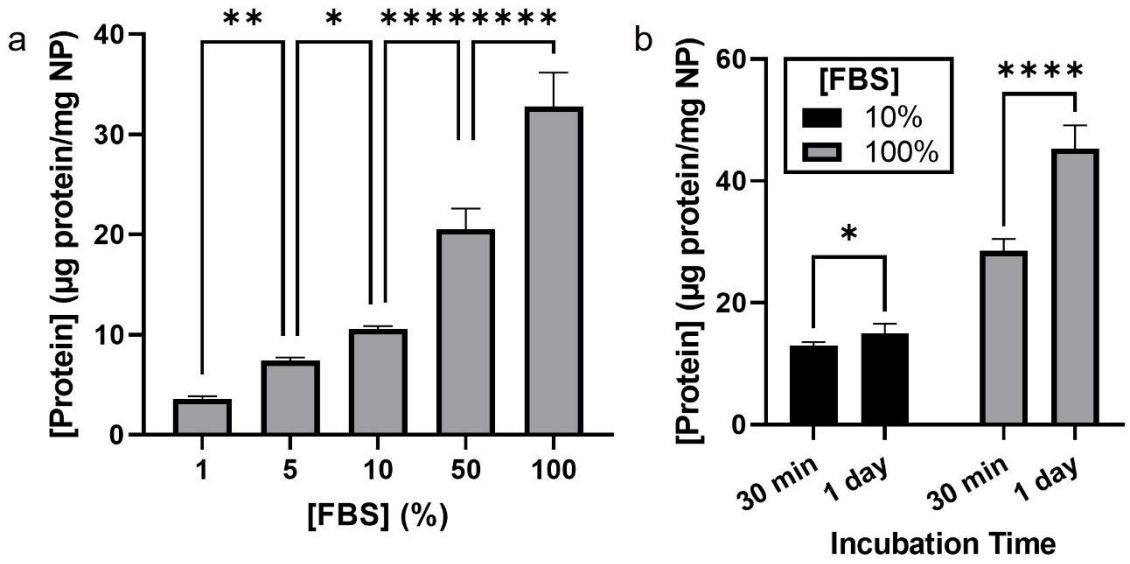

Fig. 1 Concentration of FBS adsorbed on NPs. (a) Protein adsorption as a function of initial FBS concentration used to form the protein corona. NPs were incubated with FBS for 30 min (n=6). The mean protein per NP (µg/mg) is reported. Error bars show standard deviation. Significance was calculated using an ANOVA with a post-hoc Tukey test. (b) Protein adsorption as a function of incubation time. NPs were incubated with 10% (black) or 100% (gray) FBS for either 30 min or 1 day to form a protein corona (n=6). Error bars show standard deviation. Significance was calculated using an unpaired two-sided t-test. *p<0.05, **p<0.01, ****p<0.0001

Towards low-cost proteomics: Automation and replicates

The best method to determine the composition of the protein corona is LC-MS/MS. At the Duke University core facility, and likely others, the cost of a proteomic experiment scales with the time required to run the samples. Previously, our lab compared the data generated by a lower cost, high-speed method, MicroFlow, and the standard, slower, NanoFlow [22]. We found nearly identical results for the 50 most abundant proteins observed in the protein corona, with a 4x decrease in cost per sample using MicroFlow. Our next steps in reducing costs, described below, have been to develop methods for automated sample digestion and determine the need for replicate samples.

We used commercially available S-Traps to isolate and digest the corona proteins. The process is not currently fully automated as the S-Traps must be manually moved to a

centrifuge, but S-Traps can maintain the 96-well plate format. Aside from the centrifugation steps, the digestion is performed by the liquid handling robot, decreasing the hands-on time for the researcher. The digestion requires three different incubations with multiple reagent loading steps. Without the robot, the protocol is estimated to include 25 minutes of hands-on pipetting time, 145 minutes of incubation time, and 5 minutes of centrifuge time for 8 samples. Using the robot removes the hands-on researcher time for the 25 minutes of pipetting. Adding this time saved to previously reported active time savings of 30 minutes [22], shows that 55 minutes of active pipetting time is saved during automated corona formation and digestion. The time saved increases linearly with the number of samples and also increases reproducibility by removing human pipetting errors.

We tested three aspects of experimental reproducibility relevant to proteomics (Fig. 2). Verification of the LC-MS/MS was performed using a study pool quality control (SPQC), in which all samples in each batch are pooled (study pool) and an aliquot of the study pool is injected at the beginning, middle and end of the injection run. SPQC, which is a standard quality control measure [53], verifies that the LC-MS/MS instrument does not vary as a function of injection time. To characterize possible variation due to the digest, a single sample (30 min, 10% FBS) was aliquoted (x3) and digested individually. To measure biological variability, three separate samples (30 min, 10% FBS) were digested individually.

Venn diagrams of the 50 most abundant proteins present in the coronas are used to show the variation in these samples (Fig. 2). Variation is very low. As expected, the SPQC has almost no variation with only two different proteins between the three different injection times. The variation of a triplicate digestion of a single sample is similarly low. The true biological triplicate, three individual samples, also shows very low variation with 48 of 50 proteins overlapping across all 3 samples. Overall, with the low variation in the digest and biological replicates, we are confident that digest replicates are not necessary and that biological replicates can be used to focus on specific questions of interest. Use of a single sample for proteomics has been used in other protein corona studies and may be appropriate for some *in vitro* experiments [44, 52, 54].

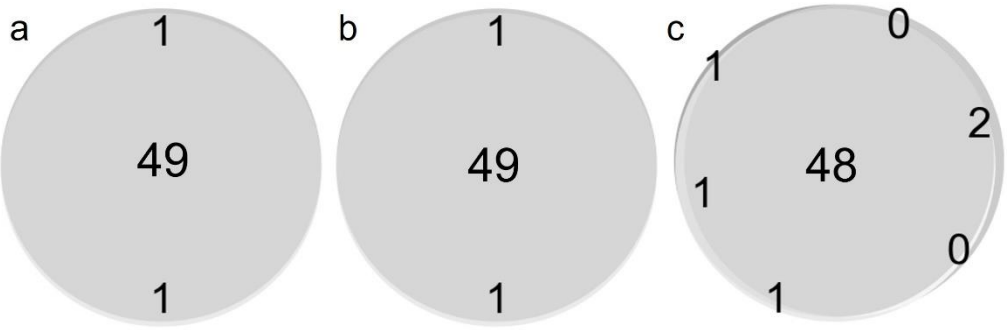

Fig. 2 Venn diagrams showing variation in proteomic data. (a) SPQC consisting of pooled samples injected at the beginning, middle, and end of the injection run. (b) Digest triplicate

obtained from a single sample digested in triplicate. (c) Biological triplicate. The Venn diagrams were created by sorting each sample by the most abundant proteins.

Composition of the protein corona: Abundance and enrichment

Proteomic analysis of protein coronas can be evaluated as the amount of protein detected (normalized abundance; Table 2) or the amount of protein in the corona relative to the amount in serum (enrichment, Fig. 3). For example, albumin is the most abundant protein in FBS comprising 36% of the protein in FBS (Table 2). It is present in the corona at high abundance (8.83 ± 2.16%). However, compared to the very high abundance of albumin in FBS, albumin is depleted in the protein corona (Fig. 3). In comparison, prothrombin (7.68 ± 0.63%), the 2nd most abundant protein in the corona, is only the 45th most abundant protein in FBS (0.05%). It is highly enriched in the protein corona (Fig. 3).

Table 2 Normalized abundance (%) for the top twenty-five most abundant corona proteins (10% FBS, 30 min incubation, n=3). For comparison, the rank order of proteins in FBS is shown in parentheses.

Protein	Protein corona (%)	FBS (%)
Albumin	8.83 ± 2.16	35.69 (1)
Prothrombin	7.68 ± 0.63	0.05 (45)
Antithrombin-III	6.84 ± 0.21	0.33 (22)
Complement factor H	5.03 ± 0.41	0.11 (37)
Plasma serine protease inhibitor	4.88 ± 1.55	0.15 (33)
Alpha-2-HS-glycoprotein (fetuin-A)	4.25 ± 1.51	26.26 (2)
Tetranectin	4.14 ± 0.16	0.08 (40)
Kininogen-1	3.56 ± 0.28	0.66 (14)
Hemoglobin subunit alpha	3.43 ± 0.05	0.46 (15)
Alpha-1-antiproteinase	3.15 ± 0.57	12.09 (3)
Gelsolin	2.88 ± 0.21	0.12 (36)
Apolipoprotein E	2.77 ± 0.05	0.02 (59)
Thrombospondin-1	2.45 ± 0.14	0.08 (41)
Hemoglobin fetal subunit beta	1.8 ± 0.01	0.28 (25)
Protein AMBP	1.71 ± 0.06	0.07 (43)
Plasma kallikrein	1.56 ± 0.14	0.04 (50)
Histidine-rich glycoprotein	1.43 ± 0.06	0.04 (48)
Kininogen-2	1.42 ± 0.03	0.26 (26)
Beta-2-glycoprotein 1	1.37 ± 0.11	0.36 (18)
Complement C4	1.37 ± 0.12	0.15 (32)
C4b-binding protein alpha chain	1.36 ± 0.04	0 (61)
Hyaluronan-binding protein 2	1.16 ± 0.13	0 (62)
Plasminogen	1.13 ± 0.09	0.21 (29)
Apolipoprotein A-I	1.08 ± 0.11	0.43 (17)
Alpha-2-macroglobulin	1.02 ± 0.08	1.26 (10)

The most abundant proteins observed in this protein corona have been detected in other corona studies [55-59], including our own [22, 54]. For example, albumin, prothrombin, antithrombin-III, complement factor H, plasma serine protease inhibitor, and alpha-2-HS-glycoprotein have been observed in the corona of carboxylate-modified polystyrene NPs (200 nm) [22, 54]. Albumin, antithrombin-III, complement factor H, and alpha-2-HS-glycoprotein were also observed in the corona of anionic TiO_2 NPs (300 nm aggregates) [54]. Complement factor H, the 4th most abundant protein in the corona (30 min, 10% FBS), is of specific interest. It has been observed in the corona of many types of NPs including silica (carboxylate-, amine-, un-modified; 30 nm,140 nm) [41], polystyrene (anionic; 112 nm) [41], and iron oxide (PEGylated, 13 nm) [60]. The presence of complement factor H in the corona has the potential to help avoid the alternative pathway response [61].

While the individual proteins in the corona have been observed in other NP studies, the enrichment or depletion of specific proteins, the “signature” of the protein corona (Fig. 3), is unique to these NPs. This highlights a general challenge in the protein corona field. While there are common corona proteins, it is impossible to predict the specific compositional signature of a protein corona based on previous studies.

A summary view of protein enrichment (or depletion) of corona proteins relative to serum proteins shows that corona composition is relatively insensitive to incubation time or initial FBS concentration (Fig. 3). Sample grouping for each protein was assessed with an outlier test (ROUT, Q=5%), resulting in two outliers, hemoglobin subunit alpha (1 day, 10% FBS) and apolipoprotein E (1 day, 100% FBS). In addition to these two outliers, tetranectin and C4b-binding protein alpha chain show differences in enrichment at 10% and 100% FBS that may be of interest for future studies. C4b-binding protein alpha chain has been noted in previous corona studies [62-65], including a high correlation with the uptake of gold NPs (10 nm) by macrophage cells [64].

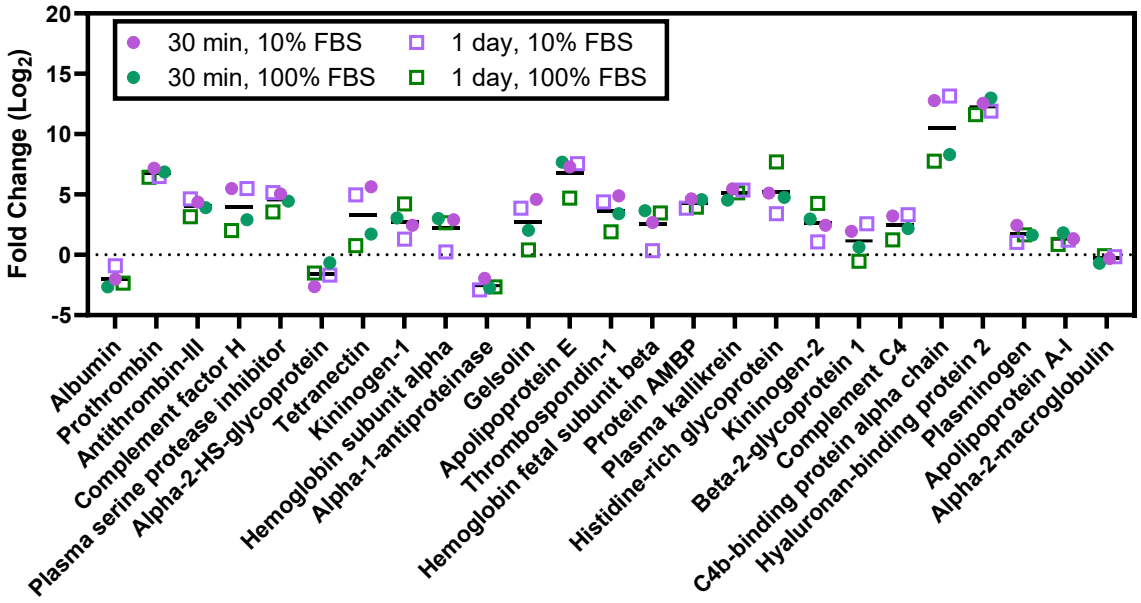

Fig. 3 Enrichment of the 25 most abundant proteins present in the corona (with top 25 based on the 30 min, 10% FBS incubation sample) relative to their abundance in FBS. Fold change, log base 2, is plotted for each protein at 30 min (filled circles) or 1 day (open squares) incubations in 10% (purple) or 100% (green) FBS.

Increasing incubation time and concentration leads to slight increases in corona differentiation

To gain an understanding of how the composition of the protein corona changes with increasing FBS concentration and time, we ran proteomic analysis of three different FBS incubation concentrations: 5%, 10%, and 100% FBS. For each concentration we examined two incubation times: 30 minutes and 1 day. Venn diagrams of the 50 most abundant proteins present in the coronas are used to illustrate the differences in the protein coronas formed following a 30 min or 1 day incubation with a 10% and 100% FBS incubation concentration (Fig. 4). Data for the 5% FBS incubation and hierarchical clustered heat maps for all samples are included in ESM (Figs. S3 - S6).

For both 10% FBS and 100% FBS incubations, the similarities in the corona following 30 min and 1 day incubations are high with 41 common proteins (of 50) for 10% FBS incubations and 37 common proteins for a 100% FBS incubation. For the most part, the proteins that do change as a function of time are relatively low in abundance. The exceptions to this are serotransferrin, which becomes the 10th most abundant protein in the 10% FBS corona after a 1 day incubation, and cadherin-1, which becomes the 13th most abundant protein in the 100% FBS corona after 1 day. Neither of these proteins were top 50 proteins following a 30 min incubation.

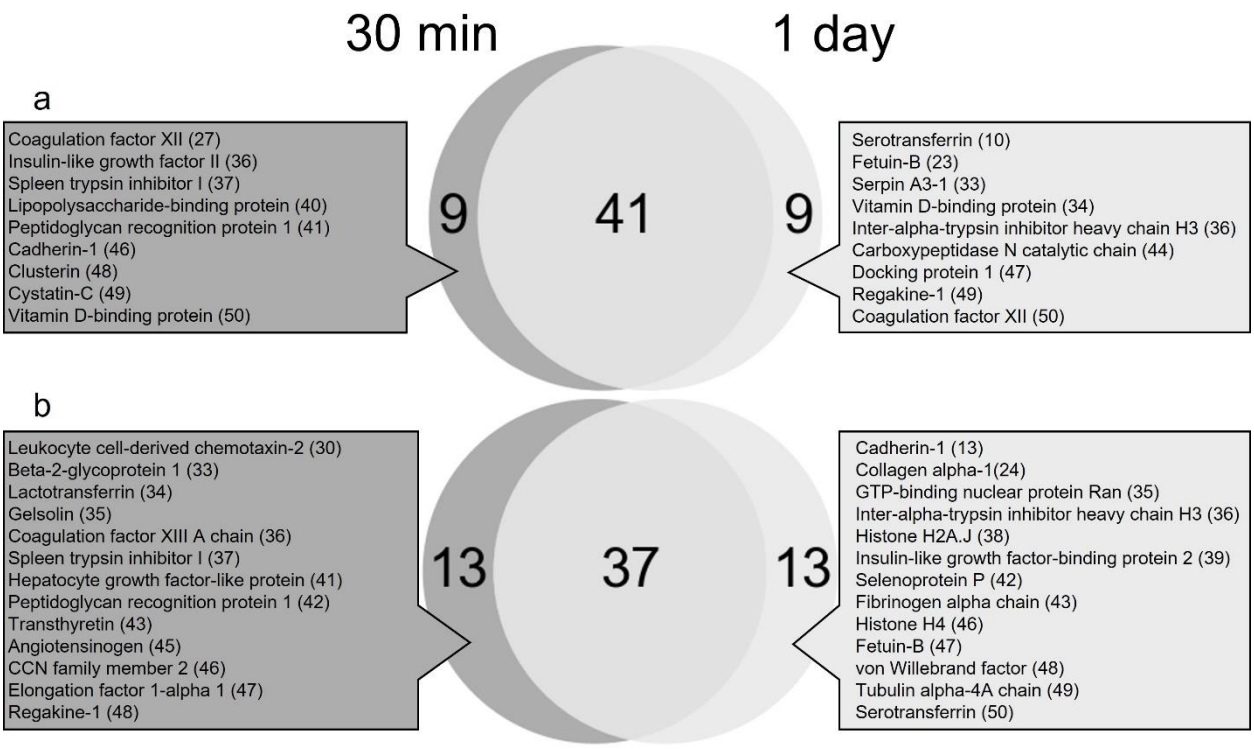

Fig. 4 Venn diagrams illustrate the differences in the top 50 most abundant proteins following 30 min and 1 day incubations. The rank of each protein is shown in parentheses. (a) 10% FBS. (b) 100% FBS. Results for 5% FBS are included in ESM (Fig. S3).

A similar approach was used to illustrate the differences in the protein coronas due to incubation concentration (Fig. 5). Protein coronas were formed following a 30 min or 1 day incubation with a 10% and 100% FBS incubation concentration. Tetranectin and C4b-binding protein alpha chain are observed in protein coronas formed with 10% FBS, but not 100% FBS. Coagulation factor XI is only observed in high abundance on protein coronas formed with 100% FBS.

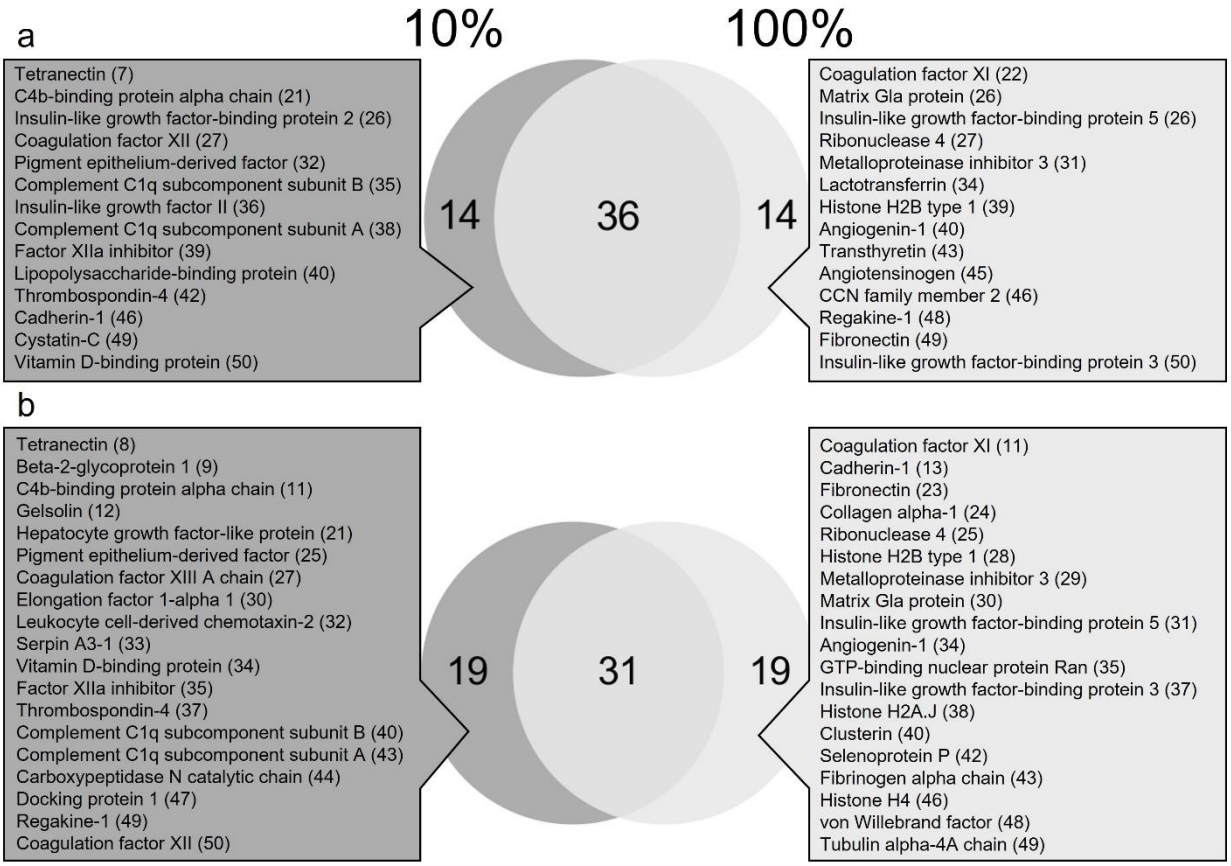

Fig. 5 Venn diagrams showing the differences in the top 50 most abundant proteins for each incubation time at each incubation concentration. (a) 30 min incubation. (b) 1 day incubation. Results for 5% FBS are included in ESM (Fig. S4).

An extensive previous proteomics study examined the corona formed on silica (35 nm, 140 nm) and polystyrene (120 nm) NPs, with a range of functional groups, including carboxylate-modified polystyrene, incubated with human plasma [41]. This research showed that the compositional signature of the protein corona was established quickly (30 s) with only the relative concentration of proteins changing over time (30 s - 480 min). Similarly, proteomic analysis of the corona formed from human plasma on polystyrene NPs (50 nm, 100 nm; amine, carboxylate, or no modification) showed no time-dependence from 5 min- 5 hr [66]. We see similar results in that few new proteins with high (~top 10) abundance are altered as a function of time.

Conclusions

We describe the automated generation, isolation, and digestion of protein coronas formed on carboxylate-modified magnetic NPs (Table 1). We use these methods to characterize the concentration and composition of the protein corona as a function of incubation time and FBS concentration. Our experiments show that increased concentrations of FBS during the formation of the protein corona led to increased concentrations of corona proteins (Fig. 1a), as a function of both incubation time and concentration (Fig. 1b). The

interdependence of time and concentration suggests possible reasons, although not a mechanism, for conflicting reports in the protein corona literature [41, 49-52].

An overarching theme of our work has been the development of methods to reduce the costs associated with protein corona experiments, including lower cost proteomics [22], and, as described here, automating the digest step typically carried out by a core facility. We also carried out triplicate experiments to measure reproducibility across LC/MS-MS experiments. We find high reproducibility among triplicate samples (Fig. 2). We also compared proteins of interest identified by gel electrophoresis to our results from proteomics with the hope of further reducing costs (Fig. S7). Unfortunately, bands of interest identified by gel electrophoresis did not correspond to results from proteomics.

Using proteomics data, we describe both the abundance (Table 2) and enrichment-depletion (Fig. 3) of the proteins adsorbed on the surface of the NPs. The composition of the protein corona shows small changes as a function of incubation time and FBS concentration (Figs. 4 and 5). The most abundant proteins are fairly insensitive to the conditions used to form the coronas.

Moving forward, this research points in two directions. The first is the use of enrichment-depletion data to select proteins for future molecular studies. The enrichment and depletion of proteins in the corona relative to the proteins present in the serum used to form the corona is a purely biophysical interaction, dependent on only the physical and chemical properties of the protein and NP. Understanding why hemoglobin subunit alpha, apolipoprotein E, tetranectin, and C4b-binding protein alpha show unique NP adsorption may help define the molecular interactions governing corona formation. Second, increasing automation and decreasing costs of protein corona characterization will help generate the large data sets necessary for machine learning approaches. We hope to stimulate future studies at both the single protein and big data levels.

Ethics Declarations

Conflicts of interest

The authors declare that they have no conflicts of interest.

Funding

This study received funding from the NSF (CBET-1901579).

Acknowledgments

The authors thank Gustavo Sosa Macias, Judith Dominguez, and Nathan Rayens for helpful discussion. We thank the Duke University School of Medicine for the use of the Proteomics and Metabolomics Shared Resource, which provided proteomics service, with special thanks to Erik Soderblom and Greg Waitt for technical advice.

Electronic Supplementary Material

An automated approach to the protein corona: Concentration and composition of the protein corona as a function of incubation time and serum concentration

Karsten M. Poulsen and Christine K. Payne*

Thomas Lord Department of Mechanical Engineering and Materials Science, Duke University, Durham, North Carolina, USA 27705

christine.payne@duke.edu

Table S1 (attached Excel spreadsheet): Complete proteomics data using the Top3 quantification, organized by sample. Tabs for FBS, Normalized abundance (%), and Fold change (log2), provide the normalized abundance (%) for the proteins observed in FBS, the normalized abundance (%) of the corona proteins observed for each incubation condition, and the fold change observed for each protein at each incubation condition. Negative infinity values in the fold change tab were replaced with zeros after enrichment calculations.

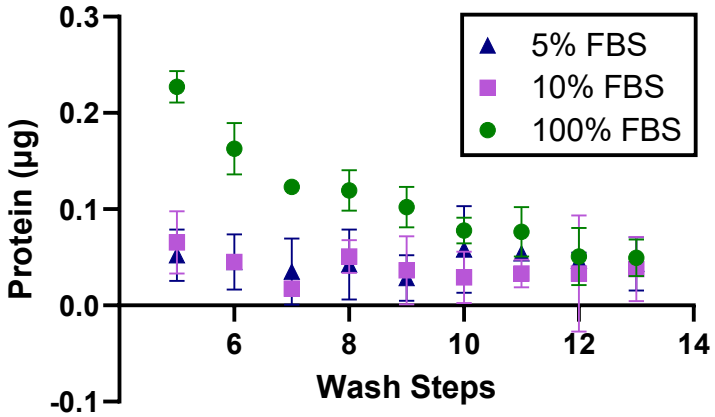

Fig. S1 Concentration of protein present in the supernatant following "washing" of protein-NP samples. Wash #5 is the first sample shown. The first 4 wash steps show much higher protein concentrations and are not typically measured. NPs were incubated with FBS for 30 min and washed by the robot (n=2). Error bars show standard deviation.

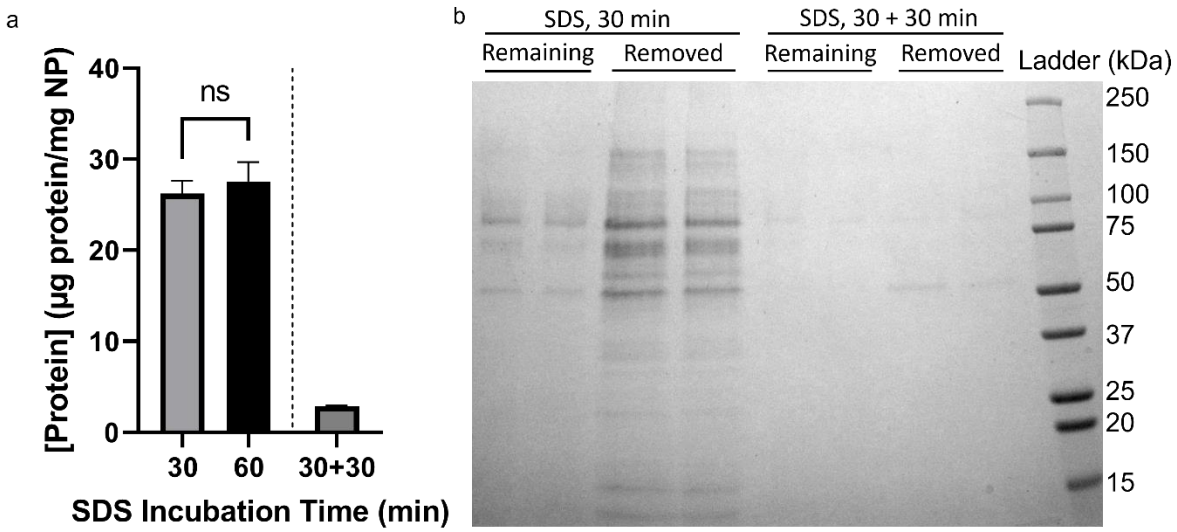

Fig. S2 Residual protein is resistant to removal by SDS. The bulk of the protein corona is removed following a 30 min SDS incubation, as described in Materials and Methods. (a) There is no significant difference in protein removal following a 30 min (light gray) or 60 min (black) incubation with SDS, measured by the 660 nm assay for coronas formed following a 30 min, 100% FBS incubation. The concentration of protein removed after two sequential 30 min SDS incubation steps (dark gray) is at the edge of the working detection limit of the assay (50 µg/mL). (b) Gel electrophoresis was used to determine if SDS led to selective protein removal. The proteins visible (Remaining) after SDS treatment (30 min) are the same as the most abundant proteins removed (Removed) by SDS. A second SDS removal step (30+30 min) shows removal of additional protein at ~50 kDa, likely albumin, and residual protein remaining at ~90 kDa. Given the non-significant difference in protein removal, a single SDS removal step was chosen to match with Proteomics Core Facility protocols.

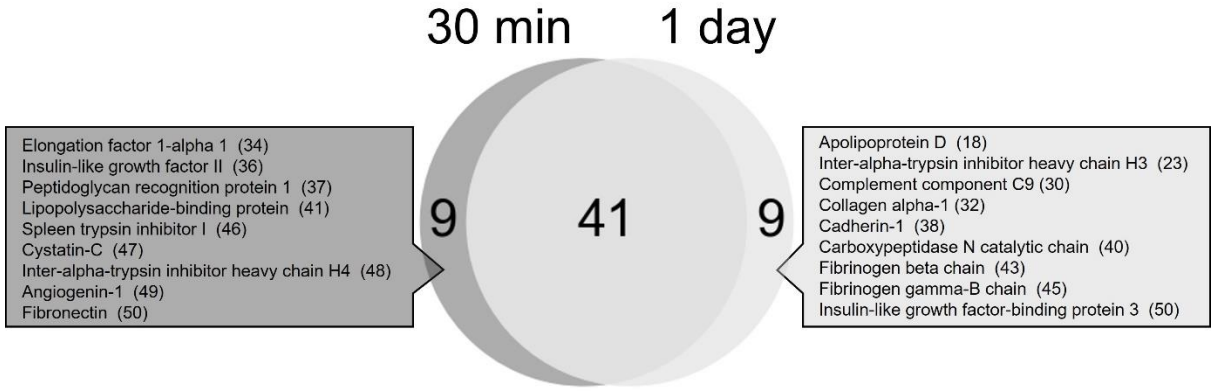

Fig. S3 Venn diagram showing the differences in the top 50 most abundant proteins following 30 min and 1 day incubations with 5% FBS incubation. Protein ranks are included in parentheses.

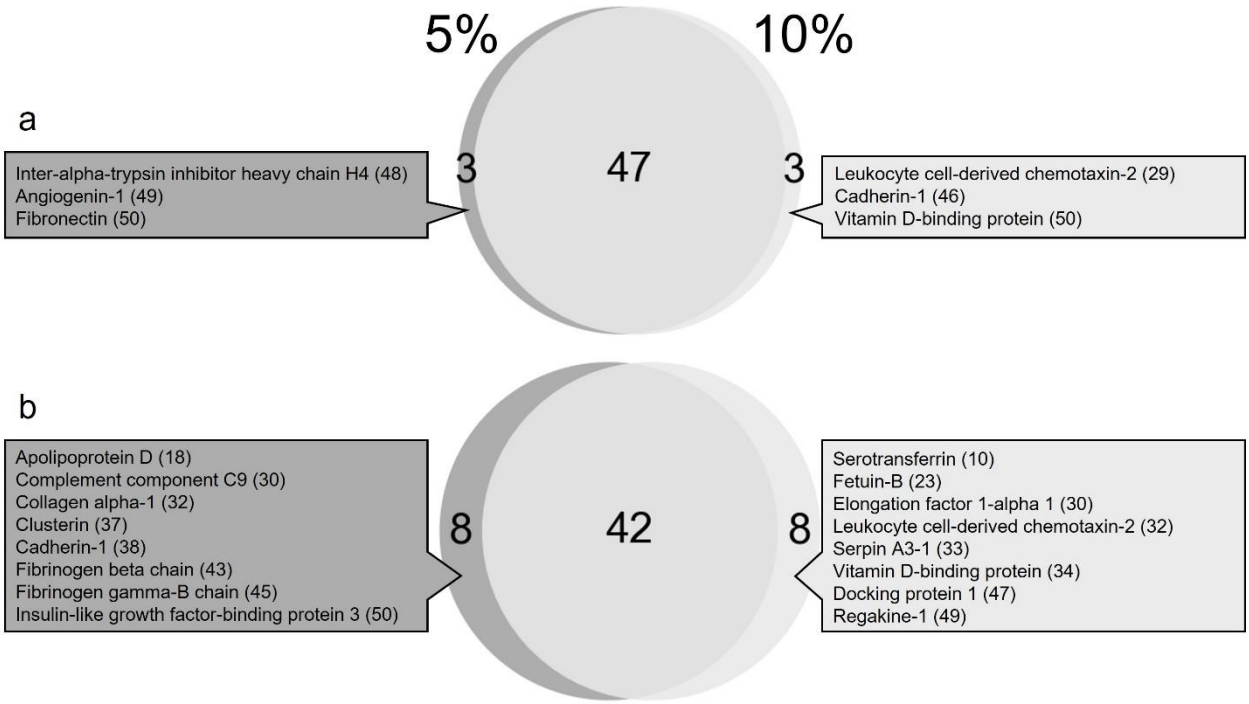

Fig. S4 Venn diagrams showing the differences in the top 50 most abundant proteins for 5% and 10% FBS incubations. (a) 30 min incubation. (b) 1 day incubation. Protein ranks are included in parentheses.

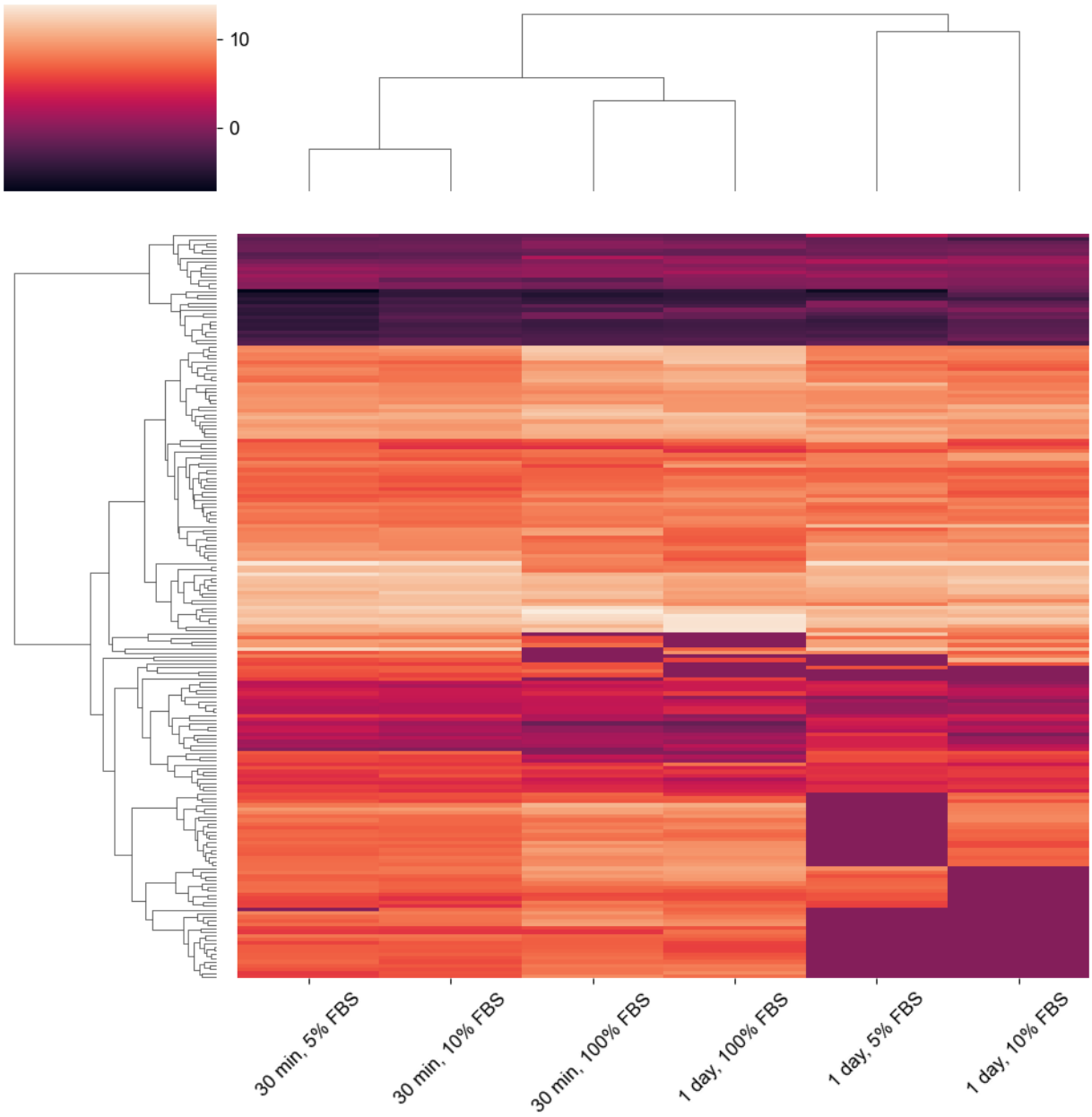

Fig. S5 Hierarchical clustered heat map of proteomics data with each incubation condition on the x-axis and individual proteins on the y-axis. Fold change data is used for the clustering. 200 proteins are displayed across 6 six different conditions. Fig. S6 shows the top 25 proteins for better visualization.

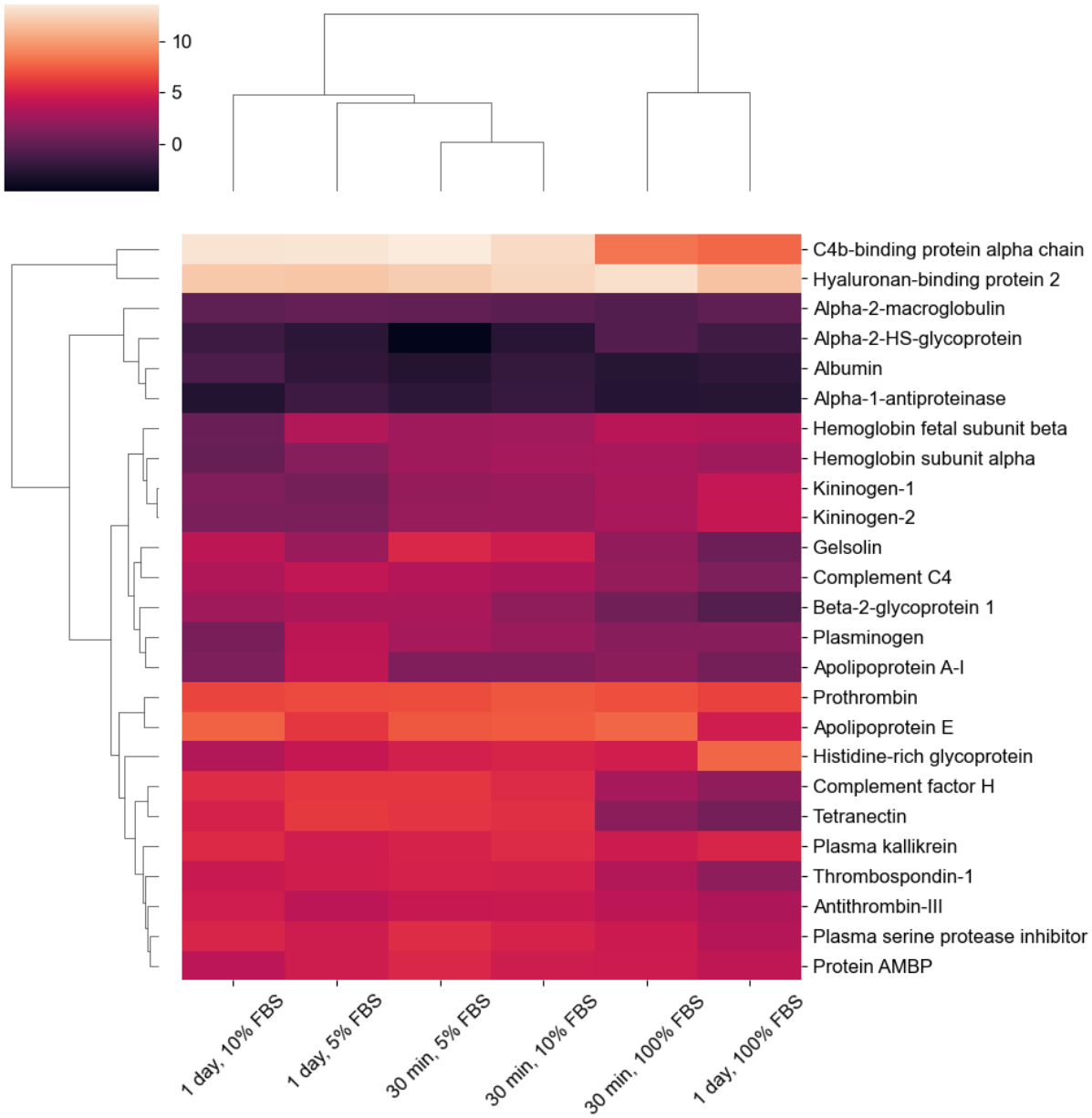

Fig. S6 Hierarchical clustered heat map of proteomics data with each incubation concentration and incubation time on the x-axis and individual proteins on the y-axis. Fold change data is used for the clustering. The top 25 proteins, ordered by the 30 min, 10% FBS sample are displayed for each incubation condition.

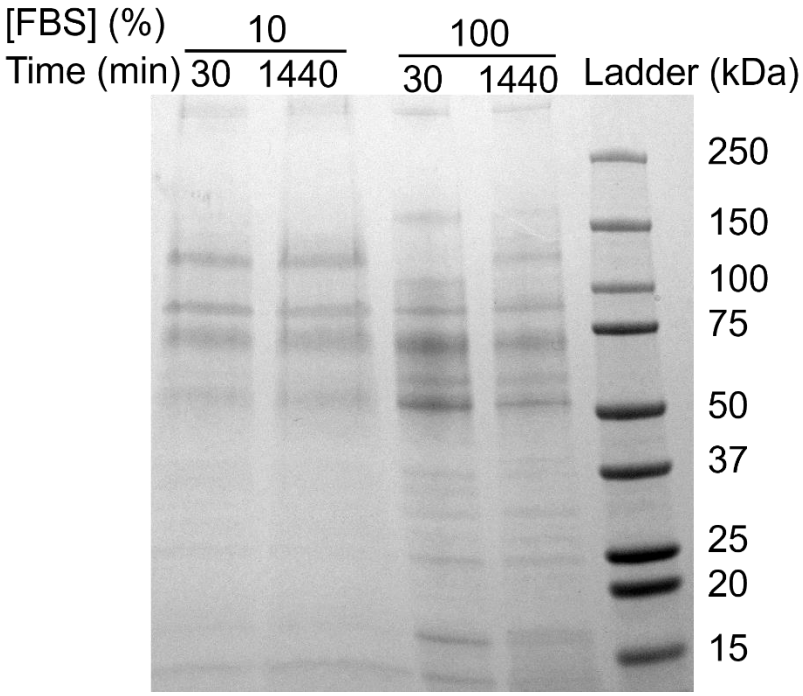

Fig. S7 Gel electrophoresis of the protein corona formed on NPs as a function of incubation time (30 min and 1 day) and FBS concentration used to form the corona (10%, and 100% FBS). Gel electrophoresis and LC-MS/MS results were compared to see if gel electrophoresis could be used as a less expensive replacement for LC-MS/MS. Gel electrophoresis shows a change in two bands as a function of incubation time and incubation concentration. A band at ~100 kDa is only visible in the 30 min, 100% FBS sample. Based on proteomics this band is likely spondin-1 (MW 91 kDa), as its normalized abundance was ~9 times greater for the 30 min, 100% FBS sample than any other sample. A band observed at ~140 kDa is visible in all of the samples except for 30 min, 100% FBS. In comparison, based on proteomics, no protein is absent from only this sample. The band at ~160 kDa was excised and confirmed to be complement C3 (MW 187 kDa) by LC/MS-MS. In agreement with the gel, complement C3 was observed in higher abundance for 100% FBS than 10% FBS by proteomics, although it is present at all FBS concentrations. Unlike results from the gel, proteomics showed the highest complement C3 abundance at 1 day. Overall, we were unable to correlate gel electrophoresis with LC/MS-MS results. We expect this is a combination of differing levels of protein staining and protein modifications. The lack of correlation between gel electrophoresis and LC/MS-MS points towards the value of working to decrease the costs of proteomics experiments.

References

1. Fleischer CC, Payne CK. Nanoparticle-cell interactions: molecular structure of the protein corona and cellular outcomes. Acc Chem Res. 2014;47:2651-9.
2. Walkey CD, Chan WC. Understanding and controlling the interaction of nanomaterials with proteins in a physiological environment. Chem Soc Rev. 2012;41:2780-99.
3. Monopoli MP, Aberg C, Salvati A, Dawson KA. Biomolecular coronas provide the biological identity of nanosized materials. Nat Nanotechnol. 2012;7:779-86.
4. Nienhaus K, Nienhaus GU. Towards a molecular-level understanding of the protein corona around nanoparticles – Recent advances and persisting challenges. Curr Opin Biomed Eng. 2019;10:11-22.
5. Kobos L, Shannahan J. Biocorona-induced modifications in engineered nanomaterial-cellular interactions impacting biomedical applications. Wiley Interdiscip Rev Nanomed Nanobiotechnol. 2020;12:e1608.
6. Tomak A, Cesmeli S, Hanoglu BD, Winkler D, Oksel Karakus C. Nanoparticle-protein corona complex: understanding multiple interactions between environmental factors, corona formation, and biological activity. Nanotoxicology. 2021;15:1331-57.
7. Abarca-Cabrera L, Fraga-Garcia P, Berensmeier S. Bio-nano interactions: binding proteins, polysaccharides, lipids and nucleic acids onto magnetic nanoparticles. Biomater Res. 2021;25:1-18.
8. Cai R, Chen C. The Crown and the Scepter: Roles of the protein corona in nanomedicine. Adv Mater. 2019;31:e1805740.
9. Payne CK. A protein corona primer for physical chemists. J Chem Phys. 2019;151:130901.
10. Docter D, Strieth S, Westmeier D, Hayden O, Gao M, Knauer SK, et al. No king without a crown – impact of the nanomaterial-protein corona on nanobiomedicine. Nanomedicine. 2015;10:503-19.
11. Frtus A, Smolkova B, Uzhytchak M, Lunova M, Jirsa M, Kubinova S, et al. Analyzing the mechanisms of iron oxide nanoparticles interactions with cells: A road from failure to success in clinical applications. J Control Release. 2020;328:59-77.
12. Ke PC, Lin S, Parak WJ, Davis TP, Caruso F. A decade of the protein corona. ACS Nano. 2017;11:11773-6.
13. Hamad-Schifferli K. Exploiting the novel properties of protein coronas: emerging applications in nanomedicine. Nanomedicine. 2015;10:1663-74.
14. Wheeler KE, Chetwynd AJ, Fahy KM, Hong BS, Tochihuitl JA, Foster LA, et al. Environmental dimensions of the protein corona. Nat Nanotechnol. 2021;16:617-29.
15. Wang D, Saleh NB, Byro A, Zepp R, Sahle-Demessie E, Luxton TP, et al. Nano-enabled pesticides for sustainable agriculture and global food security. Nat Nanotechnol. 2022;17:347-60.
16. Deng D, Li Y, Xue J, Wang J, Ai G, Li X, et al. Gold nanoparticle-based beacon to detect STAT5b mRNA expression in living cells: a case optimized by bioinformatics screen. Int J Nanomedicine. 2015;10:3231-44.
17. Verma A, Stellacci F. Effect of surface properties on nanoparticle-cell interactions. Small. 2010;6:12-21.
18. Carrillo-Carrion C, Carril M, Parak WJ. Techniques for the experimental investigation of the protein corona. Curr Opin Biotechnol. 2017;46:106-13.

19. Jayaram DT, Pustulka SM, Mannino RG, Lam WA, Payne CK. Protein corona in response to flow: effect on protein concentration and structure. Biophys J. 2018;115:209-16.
20. Pisani C, Gaillard JC, Dorandeu C, Charnay C, Guari Y, Chopineau J, et al. Experimental separation steps influence the protein content of corona around mesoporous silica nanoparticles. Nanoscale. 2017;9:5769-72.
21. Hoang KNL, Wheeler KE, Murphy CJ. Isolation Methods Influence the Protein Corona Composition on Gold-Coated Iron Oxide Nanoparticles. Anal Chem. 2022;94:4737-46.
22. Poulsen KM, Pho T, Champion JA, Payne CK. Automation and low-cost proteomics for characterization of the protein corona: experimental methods for big data. Anal Bioanal Chem. 2020;412:6543-51.
23. Zarei M, Aalaie J. Profiling of nanoparticle-protein interactions by electrophoresis techniques. Anal Bioanal Chem. 2019;411:79-96.
24. Findlay MR, Freitas DN, Mobed-Miremadi M, Wheeler KE. Machine learning provides predictive analysis into silver nanoparticle protein corona formation from physicochemical properties. Environ Sci Nano. 2018;5:64-71.
25. Ban Z, Yuan P, Yu F, Peng T, Zhou Q, Hu X. Machine learning predicts the functional composition of the protein corona and the cellular recognition of nanoparticles. Proc Natl Acad Sci U S A. 2020;117:10492-9.
26. Ouassil N, Pinals Rebecca L, Del Bonis-O'Donnell Jackson T, Wang Jeffrey W, Landry Markita P. Supervised learning model predicts protein adsorption to carbon nanotubes. Sci Adv.8:eabm0898.
27. Blume JE, Manning WC, Troiano G, Hornburg D, Figa M, Hesterberg L, et al. Rapid, deep and precise profiling of the plasma proteome with multi-nanoparticle protein corona. Nat Commun. 2020;11:3662.
28. Schneider CA, Rasband WS, Eliceiri KW. NIH Image to ImageJ: 25 years of image analysis. Nat Methods. 2012;9:671-5.
29. Cox J, Mann M. MaxQuant enables high peptide identification rates, individualized p.p.b.-range mass accuracies and proteome-wide protein quantification. Nat Biotechnol. 2008;26:1367-72.
30. Tyanova S, Temu T, Cox J. The MaxQuant computational platform for mass spectrometry-based shotgun proteomics. Nat Protoc. 2016;11:2301-19.
31. cRAP protein sequences: The Global Proteome Machine; 2012 [Available from: https://www.thegpm.org/crap/index.html.]
32. Bruckner M, Simon J, Jiang S, Landfester K, Mailander V. Preparation of the protein corona: How washing shapes the proteome and influences cellular uptake of nanocarriers. Acta Biomater. 2020;114:333-42.
33. Docter D, Distler U, Storck W, Kuharev J, Wunsch D, Hahlbrock A, et al. Quantitative profiling of the protein coronas that form around nanoparticles. Nat Protoc. 2014;9:2030-44.
34. Simon J, Kuhn G, Fichter M, Gehring S, Landfester K, Mailander V. Unraveling the in vivo protein corona. Cells. 2021;10:132.
35. Kastan Jonathan P, Dobrikova Elena Y, Bryant Jeffrey D, Gromeier M. CReP mediates selective translation initiation at the endoplasmic reticulum. Sci Adv.6:eaba0745.

36. Perez-Riverol Y, Csordas A, Bai J, Bernal-Llinares M, Hewapathirana S, Kundu DJ, et al. The PRIDE database and related tools and resources in 2019: improving support for quantification data. Nucleic Acids Res. 2019;47:D442-D50.
37. Fleischer CC, Payne CK. Nanoparticle surface charge mediates the cellular receptors used by protein-nanoparticle complexes. J Phys Chem B. 2012;116:8901-7.
38. Doorley GW, Payne CK. Nanoparticles act as protein carriers during cellular internalization. Chem Commun. 2012;48:2961-3.
39. Hill A, Payne CK. Impact of Serum Proteins on MRI Contrast Agents: Cellular Binding and T2 relaxation. RSC Adv. 2014;4:31735-44.
40. Doorley GW, Payne CK. Cellular binding of nanoparticles in the presence of serum proteins. Chem Commun. 2011;47:466-8.
41. Tenzer S, Docter D, Kuharev J, Musyanovych A, Fetz V, Hecht R, et al. Rapid formation of plasma protein corona critically affects nanoparticle pathophysiology. Nat Nanotechnol. 2013;8:772-81.
42. Alkilany AM, Lohse SE, Murphy CJ. The Gold Standard: Gold nanoparticle libraries to understand the nano–bio interface. Acc Chem Res. 2013;46:650-61.
43. Monopoli MP, Walczyk D, Campbell A, Elia G, Lynch I, Bombelli FB, et al. Physical-chemical aspects of protein corona: relevance to in vitro and in vivo biological impacts of nanoparticles. J Am Chem Soc. 2011;133:2525-34.
44. Walkey CD, Olsen JB, Song F, Liu R, Guo H, Olsen DW, et al. Protein corona fingerprinting predicts the cellular interaction of gold and silver nanoparticles. ACS Nano. 2014;8:2439-55.
45. Runa S, Lakadamyali M, Kemp ML, Payne CK. TiO2 nanoparticle-induced oxidation of the plasma membrane: Importance of the protein corona. J Phys Chem B. 2017;121:8619-25.
46. Jayaram DT, Runa S, Kemp ML, Payne CK. Nanoparticle-induced oxidation of corona proteins initiates an oxidative stress response in cells. Nanoscale. 2017;9:7595-601.
47. Partikel K, Korte R, Mulac D, Humpf HU, Langer K. Serum type and concentration both affect the protein-corona composition of PLGA nanoparticles. Beilstein J Nanotechnol. 2019;10:1002-15.
48. Grafe C, Weidner A, Luhe MV, Bergemann C, Schacher FH, Clement JH, et al. Intentional formation of a protein corona on nanoparticles: Serum concentration affects protein corona mass, surface charge, and nanoparticle-cell interaction. Int J Biochem Cell Biol. 2016;75:196-202.
49. Vroman L, Adams A, Fischer G, Munoz P. Interaction of high molecular weight kininogen, factor XII, and fibrinogen in plasma at interfaces. Blood. 1980;55:156-9.
50. Lima T, Bernfur K, Vilanova M, Cedervall T. Understanding the Lipid and Protein Corona Formation on Different Sized Polymeric Nanoparticles. Sci Rep. 2020;10:1129.
51. Casals E, Pfaller T, Duschl A, Oostingh GJ, Puntes V. Time evolution of the nanoparticle protein corona. ACS Nano. 2010;4:3623-32.
52. Pisani C, Gaillard JC, Odorico M, Nyalosaso JL, Charnay C, Guari Y, et al. The timeline of corona formation around silica nanocarriers highlights the role of the protein interactome. Nanoscale. 2017;9:1840-51.
53. Dudzik D, Barbas-Bernardos C, Garcia A, Barbas C. Quality assurance procedures for mass spectrometry untargeted metabolomics. a review. J Pharm Biomed Anal. 2018;147:149-73.

54. Runa S, Khanal D, Kemp ML, Payne CK. TiO2 nanoparticles alter the expression of peroxiredoxin antioxidant genes. J Phys Chem C. 2016;120:20736-42.
55. Yu Q, Zhao L, Guo C, Yan B, Su G. Regulating protein corona formation and dynamic protein exchange by controlling nanoparticle hydrophobicity. Front Bioeng Biotechnol. 2020;8:210.
56. Strojan K, Leonardi A, Bregar VB, Krizaj I, Svete J, Pavlin M. Dispersion of nanoparticles in different media importantly determines the composition of their protein corona. PLoS One. 2017;12:e0169552.
57. Venerando R, Miotto G, Magro M, Dallan M, Baratella D, Bonaiuto E, et al. Magnetic nanoparticles with covalently bound self-assembled protein corona for advanced biomedical applications. J Phys Chem C. 2013;117:20320-31.
58. Sakulkhu U, Maurizi L, Mahmoudi M, Motazacker M, Vries M, Gramoun A, et al. Ex situ evaluation of the composition of protein corona of intravenously injected superparamagnetic nanoparticles in rats. Nanoscale. 2014;6:11439-50.
59. de Castro CE, Panico K, Stangherlin LM, Ribeiro CAS, da Silva MCC, Carneiro-Ramos MS, et al. The Protein Corona Conundrum: Exploring the advantages and drawbacks of its presence around amphiphilic nanoparticles. Bioconjug Chem. 2020;31:2638-47.
60. Zhang T, Li G, Miao Y, Lu J, Gong N, Zhang Y, et al. Magnetothermal regulation of in vivo protein corona formation on magnetic nanoparticles for improved cancer nanotherapy. Biomaterials. 2021;276:121021.
61. Wang Z, Hood ED, Nong J, Ding J, Marcos-Contreras OA, Glassman PM, et al. Combating complement's deleterious effects on nanomedicine by conjugating complement regulatory proteins to nanoparticles. Adv Mater. 2022;34:e2107070.
62. Caracciolo G, Pozzi D, Capriotti AL, Cavaliere C, Piovesana S, La Barbera G, et al. The liposome-protein corona in mice and humans and its implications for in vivo delivery. J Mater Chem B. 2014;2:7419-28.
63. Bigdeli A, Palchetti S, Pozzi D, Hormozi-Nezhad MR, Baldelli Bombelli F, Caracciolo G, et al. Exploring cellular interactions of liposomes using protein corona fingerprints and physicochemical properties. ACS Nano. 2016;10:3723-37.
64. Saha K, Rahimi M, Yazdani M, Kim ST, Moyano DF, Hou S, et al. Regulation of macrophage recognition through the interplay of nanoparticle surface functionality and protein corona. ACS Nano. 2016;10:4421-30.
65. Naidu PSR, Norret M, Smith NM, Dunlop SA, Taylor NL, Fitzgerald M, et al. The protein corona of PEGylated PGMA-based nanoparticles is preferentially enriched with specific serum proteins of varied biological function. Langmuir. 2017;33:12926-33.
66. Zhang H, Burnum KE, Luna ML, Petritis BO, Kim JS, Qian WJ, et al. Quantitative proteomics analysis of adsorbed plasma proteins classifies nanoparticles with different surface properties and size. Proteomics. 2011;11:4569-77.